International Journal of Pharmaceutics 375 (2009) 148–154

Contents lists available at ScienceDirect

International Journal of Pharmaceutics

journal homepage: www.elsevier.com/locate/ijpharm

Pharmaceutical Nanotechnology

Polymeric nanoparticles encapsulating betamethasone phosphate with different release profiles and stealthiness

Tsutomu Ishihara[a], Tetsushi Kubota[a,b], Tesu Choi[a], Miyuki Takahashi[a], Eri Ayano[a], Hideko Kanazawa[b], Megumu Higaki[a,*]

[a] Institute of Drug Delivery Systems, Research Center for Medical Sciences, The Jikei University School of Medicine, 3-25-8 Nishi-shimbashi, Minato-ku, Tokyo 105-8461, Japan
[b] Division of Physical Pharmaceutical Chemistry, Faculty of Pharmacy, Keio University, 1-5-30 Shibakoen, Minato-ku, Tokyo 105-8512, Japan

ARTICLE INFO

Article history:
Received 16 December 2008
Received in revised form 18 March 2009
Accepted 2 April 2009
Available online 10 April 2009

Keywords:
Betamethasone disodium 21-phosphate
Biodistribution
Drug release
Nanoparticles
PEG
PLA/PLGA polymers

ABSTRACT

The purpose of this study was to engineer nanoparticles with various sustained profiles of drug release and prolonged circulation by blending poly(D,L-lactic acid)/poly(D,L-lactic/glycolic acid) (PLA/PLGA) homopolymers and poly(ethylene glycol) (PEG)-block-PLA/PLGA copolymers encapsulating betamethasone disodium 21-phosphate (BP). Nanoparticles of different sizes, drug encapsulation/release profiles, and cellular uptake levels were obtained by mixing homopolymers and block copolymers with different compositions/molecular weights at various blend ratios by an oil-in-water solvent diffusion method. The in vitro release of BP increased with nanoparticles of smaller size or of PLGA homopolymers instead of PLA homopolymers. Furthermore, the uptake of nanoparticles by macrophage-like cells decreased with nanoparticles of higher PEG content, and nanoparticles of PEG-PLGA block copolymers were taken up earlier than those of PEG-PLA block copolymers after incubation with serum. In addition, prolonged blood circulation was observed with nanoparticles of smaller size with higher PEG content, and nanoparticles of PEG-PLA block copolymers remained longer in circulation than those of PEG-PLGA block copolymers. Analysis of BP concentration in organs revealed reduced liver distribution of blended nanoparticles compared with PLA nanoparticles. This is the first study to systematically design and characterize biodegradable PLA/PLGA and PEG-PLA/PLGA-blended nanoparticles encapsulating BP with different release profiles and stealthiness.

1. Introduction

The delivery of pharmaceuticals can be improved by drug delivery systems using therapeutic colloidal nanocarriers, including polymeric nanoparticles, micelles and liposomes (Torchilin, 2005; Yih and Al-Fandi, 2006; Peer et al., 2007). In addition to being safe, these drug delivery systems must possess high loading capacity, extended circulation time and accumulation in the required pathological sites (Moghimi et al., 2001; Feng, 2004). Polymeric nanoparticles have some advantages over liposomes; it is possible for the drug release profile of polymeric nanoparticles to be modulated, and these nanoparticles are more stable in biological fluids. Additionally, the starting polymers are less expensive than phospholipids, and the manufacturing processes are simple and suitable for industrial scale up, although the use of organic solvents may lead to toxicity issues. Among the polymeric nanoparticles for controlled drug delivery, biodegradable and biocompatible poly(D,L-lactic acid)/poly(D,L-lactic/glycolic acid)/(PLA/PLGA)-based nanoparticles have been investigated as carriers for therapeutic bioactive molecules (Peracchia, 2003; Avgoustakis, 2004; Beletsi et al., 2005), since PLA/PLGA have been studied for many years and are approved by the US Food and Drug Administration for human therapy (Okada and Toguchi, 1995; Anderson and Shive, 1997; Astete and Sabliov, 2006).

On the other hand, glucocorticoids can be highly effective in treating immunological and inflammatory diseases, but their systemic application is limited because of a high incidence of serious adverse effects. Thus, we need to develop a drug delivery system with enhanced localization to the target site and sustained drug release. We previously studied PLA/PLGA nanoparticles encapsulating hydrophilic betamethasone disodium 21-phosphate (BP) at high efficiency prepared in the presence of zinc by an oil-in-water solvent diffusion method (Ishihara et al., 2005). Although these nanoparticles encapsulating BP had a strong anti-inflammatory activity (Higaki et al., 2005; Sakai et al., 2006), they were rapidly removed from circulation by the mononuclear phagocyte system (MPS), resulting in accumulation in the liver and spleen.

Alternatively, poly(ethylene glycol) (PEG) with uncharged, hydrophilic and non-immunogenic properties is an attractive material for surface modification of the nanoparticles to reduce

* Corresponding author. Tel.: +81 33 433 1111x2430; fax: +81 33 438 2557.
E-mail address: mh0402@jikei.ac.jp (M. Higaki).

0378-5173/$ – see front matter © 2009 Elsevier B.V. All rights reserved.
doi:10.1016/j.ijpharm.2009.04.001

opsonization and prevent interactions with the MPS. PLA/PLGA nanoparticles with PEG grafting escape renal exclusion and the MPS; thus, they have enhanced half-lives in plasma (Gref et al., 1994; Stolnik et al., 1994; Bazile et al., 1995; Avgoustakis, 2004; Torchilin, 2007). Furthermore, these long-circulating nanoparticles preferentially accumulate in tumors and sites of inflammation with leaky vasculature due to enhanced permeability and retention (EPR) effects (Maeda et al., 2000). This stealth capacity of PEG depends on parameters, such as the molecular weight, density, conformation and flexibility of the PEG chains (Gref et al., 1999; Mosqueira et al., 2001). In addition, the biodistribution properties of the PLA/PLGA-based stealth nanoparticles are influenced by the size of the nanoparticles and the rate of PEG loss from the nanoparticles (Gref et al., 2001; Avgoustakis et al., 2002; Vonarbourg et al., 2006). The main advantages of PEG nanoparticles compared to other long-circulating systems are their shell stability and their ability to control the release of the encapsulated compound, since PEG-PLA helps to stabilize the inner core, reduce droplet size, and encapsulate drugs. Since a major limitation of polymeric micelles is not only their relatively low loading capacity for water-soluble drugs, but also their inability to engineer PEG content, the mixtures of PLA/PLGA homopolymers and PEG-PLA/PLGA block copolymers allow for the easy adjustment of PEG content of the nanoparticles by simply mixing the appropriate amounts of polymers. This technique provides an easy means to control the colloidal properties of the nanoparticles (Quellec et al., 1999; Zambaux et al., 1999; Avgoustakis et al., 2003; Sasatsu et al., 2006; Ishihara et al., 2008). In addition, we have already developed a method by which water-soluble BP can be efficiently encapsulated in PLA/PLGA and PEG-PLA blended nanoparticles (Ishihara et al., 2009). In that study, we suggested that the PLA/PLGA homopolymers act as a reservoir of BP and the PEG-PLA block copolymers as a surfactant of the nanoparticles.

Various types of nanoparticles with different properties, such as drug encapsulation efficiency, diameter and PEG length/density on the surface can be easily prepared by controlling the blend ratio and compositions/molecular weights of polymers as previously suggested (Gref et al., 2000; Beletsi et al., 2005). Moreover, desirable nanoparticles should maintain stability and stealthiness in the blood circulation to exhibit an EPR effect, and encapsulated drugs should be able to be released at the target site at the appropriate time, regardless of whether the nanoparticles are degraded or incorporated into the target cells.

In the present study, we prepared various PLA/PLGA-based blended PEG nanoparticles containing BP for the treatment of immunological/inflammatory diseases and evaluated the drug encapsulation/release and cellular uptake of these compounds. We also examined the blood clearance and biodistribution of nanoparticles with different release profiles and stealthiness.

2. Materials and methods

2.1. Materials

Poly(D,L-lactic acid) (PLA) and poly(D,L-lactic/glycolic acid) (PLGA) with a lactic/glycolic acid ratio of 50/50 were purchased from Wako Pure Chemicals Industries, Ltd. (Osaka, Japan). The molecular weights of the polymers were determined using gel permeation chromatography. The composition was shown to be PLGA (Mw kD) or PLA (Mw kD). The carboxyl group content of the polymers was determined fluorometrically using 9-anthryldiazomethane (Ishihara et al., 2009).

Poly(ethylene glycol)-*block*-poly(D,L-lactide) (PEG-PLA) and poly(ethylene glycol)-*block*-poly(D,L-lactide-co-glycolide) (PEG-PLGA) were synthesized by a ring-opening polymerization of D,L-lactide and glycolide (Purac America, IL, USA), which had been purified by recrystallization in ethyl acetate, in the presence of monomethoxy-PEG (5580 kDa, Mn5390; NOF Co., Tokyo, Japan) according to a previously reported method (Riley et al., 2001; Yoo and Park, 2001). The composition and molecular weight of the block copolymers were evaluated by ^{1}H-NMR and gel permeation chromatography. The composition was shown to be PEG (Mw kD)-PLA (Mw kD) and PEG (Mw kD)-PLGA (Mw kD). Molar ratios of lactic acid (LA), glycolic acid (GA), and ethylene oxide (EO) in the block copolymers were determined by ^{1}H-NMR analysis. BP, Pluronic F68, diethanolamine (DEA), and acetonitrile were obtained from Sigma Chemical Co. (MO, USA). Zinc chloride, Tween 80, rhodamine B isothiocyanate (rhodamine), 4% paraformaldehyde phosphate buffer solution, and triethylamine were purchased from Wako Pure Chemicals. Hoechst 33258 was purchased from Invitrogen (Carlsbad, CA, USA).

All reagents were dissolved in distilled water (DW), unless otherwise noted. A time-resolved fluoroimmunoassay (TR-FIA) kit for betamethasone was supplied by Shionogi & Co., Ltd. (Osaka, Japan) and the concentration of BP was calculated from that of betamethasone.

2.2. Preparation of nanoparticles

Nanoparticles were prepared by the oil-in-water solvent diffusion method as reported previously (Ishihara et al., 2009). A mixture (50 mg) of homopolymers and block copolymers was dissolved in 1 ml of acetone. The blending ratio of homopolymers and copolymers is shown as the relative % of PEG-copolymers in the blend. To this mixture, 500 μl of 7.5 mg/ml DEA in acetone, 68 μl of 1 M zinc chloride (pH 1.9), and 28 μl of 350 mg/ml BP was added in order and allowed to stand for 30 min at room temperature. A 26-G needle was used to add the mixture dropwise to 25 ml of DW stirred at 1000 rpm at a rate of 48 ml/h. During diffusion of the organic solvent into the water, nanoparticles formed rapidly along with the solidification of polymers. A combination of 1 ml of 0.5 M citrate (pH 7.0) and 125 μl of 200 mg/ml Tween 80 were immediately added to chelate BP-zinc complexes and enhance the stable dispersion of the nanoparticles, respectively. Finally, the nanoparticles were purified and concentrated by ultrafiltration (Centriprep YM-50, Amicon, Millipore, Bedford, MA, USA). Conventional PLA nanoparticles formed from homopolymers alone were also prepared by the addition of 50 mg PLA (16 kD) in 4.5 ml of acetone, 7.5 mg DEA in 500 μl of acetone, 68 μl of 1 M zinc chloride and 28 μl of 350 mg/ml BP to 0.5% Pluronic F68, as previously reported (Ishihara et al., 2005).

PLA-rhodamine conjugate was synthesized as described previously (Ishihara et al., 2009). In brief, synthesized PLA-ethylenediamine was mixed with rhodamine in DMSO and the resulting PLA-rhodamine was then purified by precipitation in isopropanol. The conjugate contained 7.2 nmol of rhodamine in 1 mg, as determined by UV–vis spectrometry. Furthermore, nanoparticles with rhodamine were formed using 1 mg of PLA-rhodamine in addition to 25 mg of PLA.

2.3. Size and encapsulation efficiency of nanoparticles

The particle size and distribution were determined by the dynamic light scattering method (FPAR-1000, Otsuka Electronics, Ltd., Osaka, Japan), and the weighted average diameter was calculated by Marquadt's method.

To determine the total BP content, a 50-μl aliquot of sample was dissolved in 450 μl of acetonitrile, and 1 ml of EDTA (50 mM, pH 7.0) was added to chelate zinc and dissolve BP. On the other hand, another aliquot of sample diluted with the same volume of EDTA (50 mM, pH 7.0) was centrifuged with an Ultrafree-MC centrifugal filter unit with PL-30 (Millipore) at 5000 × *g* for 30 min to obtain the filtrate. The BP content was determined by HPLC with a ZORBAX

Eclipse XDB-C18 column (2.1 mm × 150 mm, Agilent) using 0.1 M triethylamine/acetic acid (pH 7.0)–acetonitrile (90:10) as an eluent. The flow rate was 0.2 ml/min at 20 °C and detected at 240 nm. The drug loading of BP in the nanoparticles was defined as the ratio of the calculated (total – filtrate) content of BP to the total weight of freeze-dried nanoparticles.

The content of encapsulated dyes was also determined by HPLC with a Cymmetry 300™ C4 column (2.1 mm × 150 mm, Waters, Milford, MA, USA) for rhodamine detection using using 0.1 M triethylamine/acetic acid (pH 7.0)–acetonitrile (90:10) as an eluent. The flow rate was 0.2 ml/min at 20 °C and detected at 560 nm.

2.4. In vitro drug release

The nanoparticle solution was dissolved in a mixture of fetal bovine serum (FBS) and phosphate-buffered saline (PBS) (v/v; 1/1) at 50 μg/ml of BP. After incubation at 37 °C for the indicated time, an aliquot (100 μl) was treated with 1 μl of alkaline phosphatase (2.7 units/ml, from calf intestine, Toyobo, Tokyo, Japan) at 37 °C for 30 min to dephosphorylate BP released from the nanoparticles. Then, 300 μl of acetonitrile was added to dissolve nanoparticles and the mixture was incubated at 65 °C for another 30 min. Finally, 600 μl of 50 mM EDTA (pH 7.0, including 8.3 μg/ml anilium chloride as an internal standard for HPLC analysis) was added and the mixture was incubated for 30 min at 65 °C. After centrifugation at 12,000 × *g* for 5 min, the BP and betamethasone content in the supernatant was determined by HPLC. The release rate of BP was then defined as the ratio of released BP (measured betamethasone in supernatant) to encapsulated BP (measured BP in supernatant).

2.5. Cellular uptake of nanoparticles

RAW264.7 cells (a murine macrophage-like cell line) seeded at 1.0×10^5 cells per well (6-well cell culture plate, Costar, France) were cultured overnight in modified Eagle's medium (MEM) containing 10% heat-inactivated FBS and 100 units of penicillin, 100 μg/ml streptomycin, and 2 mM glutamine (Invitrogen) at 37 °C in a humidified atmosphere of 5% CO_2. The cells were washed with PBS and incubated with nanoparticles labeled with 5 ng/ml of rhodamine in fresh medium for 3 h at 37 °C. Then, the cells were washed 4 times with PBS and nuclei were stained with Hoechst 33258. Following fixation in 4% paraformaldehyde, intracellular localization of nanoparticles was visualized using a fluorescence microscope (Keyence BZ-9000, Keyence Co., Osaka, Japan).

The cellular uptake of nanoparticles was also determined to quantify the internalized BP in RAW264.7 cells. Nanoparticles containing 50 μg/ml BP were preincubated with 50% FBS in PBS for the indicated time at 37 °C, and then 50 μl of the preincubated nanoparticles was added to each well, which contained 1.5×10^5 RAW cells in 450 μl of fresh medium. After 3 h at 37 °C, the cells were washed 4 times with PBS and lysed with 150 μl of culture lysis reagent (Promega Co., WI, USA). Then, 300 μl of acetonitrile and 600 μl of DW were added. This solution was centrifuged at 1500 × *g* for 30 min, and the supernatant was then dried with a centrifugal evaporator. The dried pellet was treated with alkaline phosphatase, and the concentration of BP was determined by TR-FIA. The number of viable cells was determined using a cell counting kit (Dojindo Co., Kumamoto, Japan).

2.6. Animal experiments

2.6.1. In vivo blood clearance

Female 7- to 8-week-old ddY mice were purchased from Japan SLC, Inc. (Shizuoka, Japan). The experimental protocols were approved by the Jikei University Animal Care Committee in accordance with the Guide for the Care and Use of Laboratory Animals. The mice ($n = 5$ in each group) were injected in the tail vein with nanoparticles (50 μg of BP/200 μl saline), and blood was collected at the indicated time from the retro-orbital plexus of ether-anesthetized mice. Then 180 μl of acetonitrile and 360 μl of DW were added to 60 μl of blood. After centrifugation at 5000 × *g* for 10 min, 200 μl of supernatant was dried with a centrifugal evaporator for 70 min at 50 °C. The concentration of BP was determined by TR-FIA. The detection limit was 0.010 μg/ml of blood.

2.6.2. Biodistribution

After nanoparticles encapsulating BP were intravenously administered to 7-week-old female ddY mice, the tissue distribution was determined. Mice ($n = 4$ in each group) were injected in the tail vein with nanoparticles (50 μg of BP/200 μl saline). The mice were anesthetized and sacrificed by cervical dislocation after 24 h. The main tissues (liver, spleen, kidney, lung, and muscle) were excised and washed quickly with cold water to remove surface blood; then the BP contents were assayed by TR-FIA.

2.7. Statistical analysis

The Student's *t*-test and Dunnett test were used for the statistical analysis of the experimental data. Values of $p < 0.01$ were considered to indicate statistical significance.

3. Results and discussion

3.1. Characteristics of nanoparticles

The basic properties of the polymers used are shown in Table 1. Since PLA/PLGA homopolymers were obtained by condensation polymerization of lactic acid/glycolic acid, the carboxyl group content in the polymers decreased with a increase of molecular weight of homopolymers, which indicated the presence of carboxyl groups at the end of the PLA/PLGA homopolymers. On the other hand, block polymers possessed few carboxyl groups, as they were synthesized by ring-opening polymerization of D,L-lactide/glycolide in the presence of monomethoxy-PEG.

Furthermore, various types of nanoparticles encapsulating BP were prepared from different mixtures of PLA/PLGA homopolymers and PEG-PLA/PLGA block copolymers by the solvent diffusion method. The physicochemical characteristics of the nanoparticles are shown in Table 2. The diameter of the nanoparticles increased with lower PEG content in the mixtures and the diameters were similar (97–125 nm) at a same blend ratio (10%), since PEG-copolymers act as surfactants.

The composition of the mixtures influenced the drug loading of the nanoparticles, by affecting the molecular weight of polymers and the size of the nanoparticles. In nanoparticles of the same PEG content, the drug loading of BP decreased with the increased molecular weight (6 kD to 16 kD) of the PLA/PLGA homopolymers, although little difference in drug loading was observed with different molecular weights (15–28 kD) of PLA/PLGA in block polymers. Furthermore, the drug loading decreased as the PEG content of the nanoparticles increased, when nanoparticles were prepared from mixtures of PLA (6 kD) and PEG (6 kD)-PLA (9 kD) with various PEG content (5–40%). In general, large-sized particles encapsulated drugs at high efficiency because of a decrease in surface area. However, the drug loading of nanoparticles prepared from block copolymers alone (PEG-PLA micelles) was very low (0.15% in PEG(6)-PLA(30) nanoparticles with a diameter of 68 nm).

We already reported that zinc can create an ionic bridge between a carboxyl group located at the end of PLA/PLGA homopolymers and a phosphate group of BP, as BP is efficiently encapsulated in blended nanoparticles in the presence of zinc and carboxyl groups

Table 1
Polymer properties.

Polymers[a]	Mw[b]	Mn[b]	Mw/Mn	COOH[c] (μmol/g)	LA/GA/EO[d] (molar ratio)
PLA(6)	6,170	3,300	1.87	394	–
PLA(10)	10,050	4,610	2.18	298	–
PLA(16)	16,440	6,120	2.69	201	–
PLGA(6)	5,820	3,290	1.77	410	–
PLGA(9)	8,870	4,640	1.91	288	–
PLGA(16)	15,590	6,590	2.37	209	–
PEG(6)-PLA(9)	15,010	12,300	1.22	13	31/0/69
PEG(6)-PLA(16)	22,370	15,550	1.44	15	50/0/50
PEG(6)-PLA(22)	27,610	18,730	1.47	11	61/0/39
PEG(6)-PLA(30)	36,040	19,640	1.84	21	79/0/21
PEG(6)-PLGA(10)	15,550	9,820	1.58	46	22/21/57
PEG(6)-PLGA(16)	22,410	11,050	2.03	38	31/27/42
PEG(6)-PLGA(19)	25,090	12,280	2.04	33	34/32/34

[a] PLGA with a lactic/glycolic acid ratio of 50/50. PEG-PLA/PLGA block copolymers were synthesized by ring-opening polymerization of D,L-lactide and glycolide in the presence of monomethoxy-PEG (Mw, 5580; Mn, 5390).
[b] Molecular weights were determined by gel permeation chromatography.
[c] The carboxyl group content of the polymers was determined fluorometrically using 9-anthryldiazomethane.
[d] Molar ratios of lactic acid (LA), glycolic acid (GA), and ethylene oxide (EO) in the block copolymers were determined by ^{1}H-NMR analysis.

(Ishihara et al., 2009). The carboxyl groups of PLA/PLGA homopolymers may determine encapsulation of BP as a reservoir, since the drug loading of BP parallels the content of carboxyl groups in the blended polymers. In summary, good drug loading of BP in blended nanoparticles was obtained with PLA/PLGA homopolymers of lower molecular weight and with PEG-PLA/PLGA block polymers of lower blend ratio.

3.2. In vitro drug release

Since the release behavior of drugs from biodegradable particles is influenced by factors such as temperature, ionic strength, pH and the presence of biological components, we evaluated both BP release behavior and cellular uptake of nanoparticles in diluted serum (FBS/PBS, 50%, v/v, pH 7.2) at 37 °C in this study. As released BP was readily dephosphorylated by phosphatase, we could distinguish released BP from remaining BP in nanoparticles without purification. When nanoparticles were prepared by altering the blend ratio of PLA (6 kD) and PEG(6 kD)-PLA(9 kD), smaller nanoparticles with higher PEG (40% compared to 5%) exhibited gradually increased leakage, as shown in Fig. 1A, whereas conventional non-stealth PLA(16 kD) nanoparticles (type NS) hardly released BP over the 60-days observation period. The introduction of PEG into the matrix might have caused increased water uptake, leading to increased degradation compared to native PLA nanoparticles. Blended nanoparticles of similar size with 10% PEG formed from PLGA or PLA homopolymers of a low molecular weight (6 kD) tended to release BP faster than those formed from homopolymers of a high molecular weight (16 kD), as shown in Fig. 1B. Since the glass-transition temperature (Tg) depends on the molecular weight of polymers, nanoparticles of lower molecular weight homopolymers showed faster release. On the other hand, the molecular weight of PLA (9–30 kD) and the composition of PLA or PLGA in the block copolymers did not significantly affect the BP release profile (data not shown). Furthermore, blended nanoparticles formed from PLA homopolymers had a slower drug release than those from PLGA homopolymers of the same molecular weight, as shown in Fig. 1B. Since the Tg of PLA is higher than that of PLGA, nanoparticles of PLA showed lower hydrolysis than nanoparticles of PLGA in this study. Moreover, the gradual release of BP without

Table 2
Nanoparticle characteristics.

Type	PLA/PLGA (Mw)/PEG-PLA/PLGA (Mw)	Relative PEG in the blend (%)	BP loading (wt%)	Diameter (nm)
A	PLA(6)/PEG(6)-PLA(9)	5	12.7 ± 1.1	137 ± 11
	PLA(6)/PEG(6)-PLA(9)	10	10.7 ± 1.0	116 ± 10
	PLA(6)/PEG(6)-PLA(9)	20	9.9 ± 0.8	85 ± 8
	PLA(6)/PEG(6)-PLA(9)	30	7.8 ± 0.4	62 ± 6
B	PLA(6)/PEG(6)-PLA(9)	40	4.9 ± 0.5	51 ± 7
	PLA(6)/PEG(6)-PLA(16)	10	10.3 ± 1.5	97 ± 8
	PLA(6)/PEG(6)-PLA(22)	10	8.3 ± 0.8	103 ± 9
	PLA(10)/PEG(6)-PLA(9)	10	8.3 ± 0.7	107 ± 11
	PLA(16)/PEG(6)-PLA(9)	10	4.7 ± 0.6	122 ± 15
	PLA(6)/PEG(6)-PLGA(10)	5	11.7 ± 0.8	140 ± 12
C	PLA(6)/PEG(6)-PLGA(10)	10	11.2 ± 0.9	115 ± 7
	PLA(6)/PEG(6)-PLGA(10)	20	9.0 ± 0.4	96 ± 9
	PLA(6)/PEG(6)-PLGA(10)	30	5.8 ± 0.6	66 ± 5
	PLA(6)/PEG(6)-PLGA(10)	10	10.1 ± 0.8	112 ± 14
	PLA(6)/PEG(6)-PLGA(19)	10	7.9 ± 0.6	107 ± 9
D	PLGA(6)/PEG(6)-PLA(9)	10	11.4 ± 1.0	101 ± 9
	PLGA(9)/PEG(6)-PLA(9)	10	8.4 ± 0.4	113 ± 12
	PLGA(16)/PEG(6)-PLA(9)	10	5.3 ± .0.6	125 ± 13
NS	PLA(16)/ –	0	4.8 ± 1.0	178 ± 18
	– /PEG(6)-PLA(9)	58	0.03 ± 0.01	29 ± 4
	– /PEG(6)-PLA(16)	38	0.05 ± 0.02	35 ± 4
	– /PEG(6)-PLA(22)	28	0.11 ± 0.03	45 ± 6
	– /PEG(6)-PLA(30)	14	0.15 ± 0.05	68 ± 9

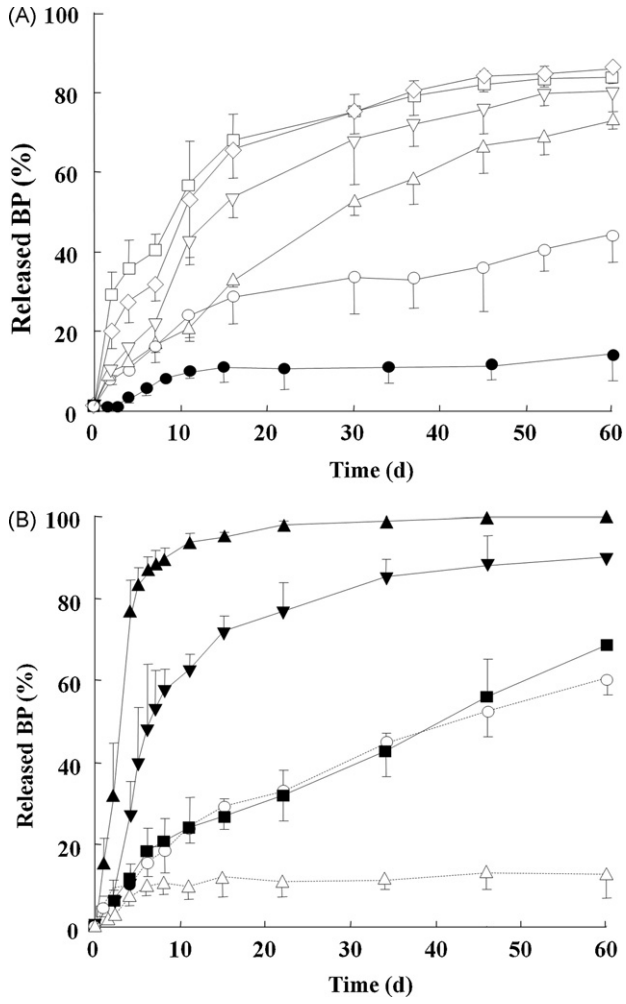

Fig. 1. Release profiles of BP from nanoparticles in 50% FBS at 37 °C. Each data point and bar represents the mean and S.D. of triplicate values. (A) PLA(6)/PEG(6)-PLA(9) and PLA(16) nanoparticles of different PEG content. (B) PEG(6)-PLA(9)-based nanoparticles with 10% PEG content.

an initial burst suggested complete incorporation of BP into the nanoparticles rather than adsorption to the particle surface.

These results indicate that the release rate of BP from nanoparticles could be controllable by changing the compositions/molecular weight of the PLA/PLGA homopolymers and the blend ratio of homopolymers and block copolymers.

3.3. Cellular uptake

The internalization of rhodamine-labeled nanoparticles into RAW cells after 3 h is shown in Fig. 2A. PLA (6)/PEG(6)-PLA(9) blended nanoparticles with 10% PEG (type A) did not internalize into cells at 3 h, whereas type NS nanoparticles internalized into cells even without serum. The Z-potential values of type A nanoparticles were close to neutral, whereas type NS nanoparticles had a highly negative Z-potential (data not shown). Meanwhile, type A nanoparticles could internalize into cells after preincubated with 50% serum for 3 days. The internalization of type NS nanoparticles was partly inhibited with chlorpromazine (data not shown), which might suggest the involvement of clathrin-mediated endocytosis, as previously reported (Panyam et al., 2002).

The amount of BP internalized into RAW cells is shown in Fig. 2B and C. Since blended nanoparticles of PLGA homopolymers (such as type D) quickly released BP in vitro, the uptake of blended nanoparticles formed from PLA homopolymers, but not PLGA homopolymers, are shown. The type NS nanoparticles internalized into cells in a short period and were not affected by the preincubation period with 50% serum, although both PLA(6)/PEG(6)-PLA(9) and PLA(6)/PEG(6)-PLGA(10) nanoparticles internalized into the cells in a preincubation-time dependent manner (Fig. 2B and C). In addition, the internalization of both PLA(6)/PEG(6)-PLA(9) and PLA(6)/PEG(6)-PLGA(10) nanoparticles decreased with increased PEG content (5–40% and 5–30%, respectively) (Fig. 2B and C). PEG was supposed to be time-dependently released from the surfaces of the nanoparticles with serum. Control free BP was not detectable inside the cells in this assay (Fig. 2C). The more rapid change of endocytic properties following preincubation was seen in nanoparticles formed with PEG-PLGA block copolymers (Fig. 2C) than those formed from PEG-PLA block copolymers (Fig. 2B). As they had the same diameter and initial PEG surface density, it appears that the PLGA-PEG block copolymers might lose their PEG chains more rapidly than PLA-PEG block copolymers. On the other hand, the different molecular weights of PLGA or PLA in the block copolymers did not affect cellular uptake (data not shown). This result implies that the length of PLA/PLGA segments in block copolymers does not affect PEG retention, as PEG release may occur by hydrolysis of the PLA/PLGA segment in block polymers. The cellular uptake in vitro can be controlled by PEG density depending on the blend ratios of homopolymers and block polymers, and by PEG loss depending on block polymer composition.

Although it appears that the blended nanoparticles in the serum initially released PEG from their surfaces, resulting in increased cellular internalization, the involvement of opsonin in serum has not yet been completely ruled out in this study (Gref et al., 2000; Nguyen et al., 2003; Vonarbourg et al., 2006).

3.4. Blood clearance and biodistribution

The size of long-circulating particles, providing that they are rigid structures, should be in the range of 120–200 nm in diameter to substantially avoid particle trapping in the space of Disse and hepatic parenchyma and splenic filtration (Moghimi et al., 2001).

The blood clearance of representative nanoparticles is shown in Fig. 3. All blended nanoparticles exhibited prolonged residence in the blood circulation compared to conventional non-stealth nanoparticles. Nanoparticles with smaller size and higher PEG content (type B) remained in the blood for an extended amount of time (half-life, $t_{1/2}$: 25.2 h). Increased PEG density resulted in a more effective steric barrier on the nanoparticle surface, inhibiting the opsonization and phagocytosis of the nanoparticle. The types A and D nanoparticles had a similar profile ($t_{1/2}$: 7.8 h and 5.8 h, respectively), indicating that the different compositions of homopolymers (PLGA or PLA) did not affect blood clearance. Type C PEG-PLGA nanoparticles with a half-life of 3.2 h might have detached PEG earlier than type B PEG-PLA nanoparticles. Type NS nanoparticles and free BP had very fast clearance ($t_{1/2}$: <10 min).

Markedly increased blood circulation time and reduced liver uptake of PEGylated PLA/PLGA nanoparticles compared to non-PEGylated nanoparticles after intravenous administration to mice has previously been demonstrated (Gref et al., 1994; Bazile et al., 1995; Stolnik et al., 2001). It has also been reported that a long PEG chain and high PEG surface density are necessary to produce an increased half-life of nanoparticles of PLA and PLA-PEG mixtures in vivo (Mosqueira et al., 2001).

In the present study, the biodistribution properties of the nanoparticles were influenced by surface PEG content, the size of the nanoparticles and the rate of PEG loss from the nanoparticles. As shown in Fig. 4, conventional type NS nanoparticles accumulated in the liver 24 h after intravenous administration. However, the accumulation of blended nanoparticles (types A–D) in the liver decreased significantly as compared to type NS nanoparti-

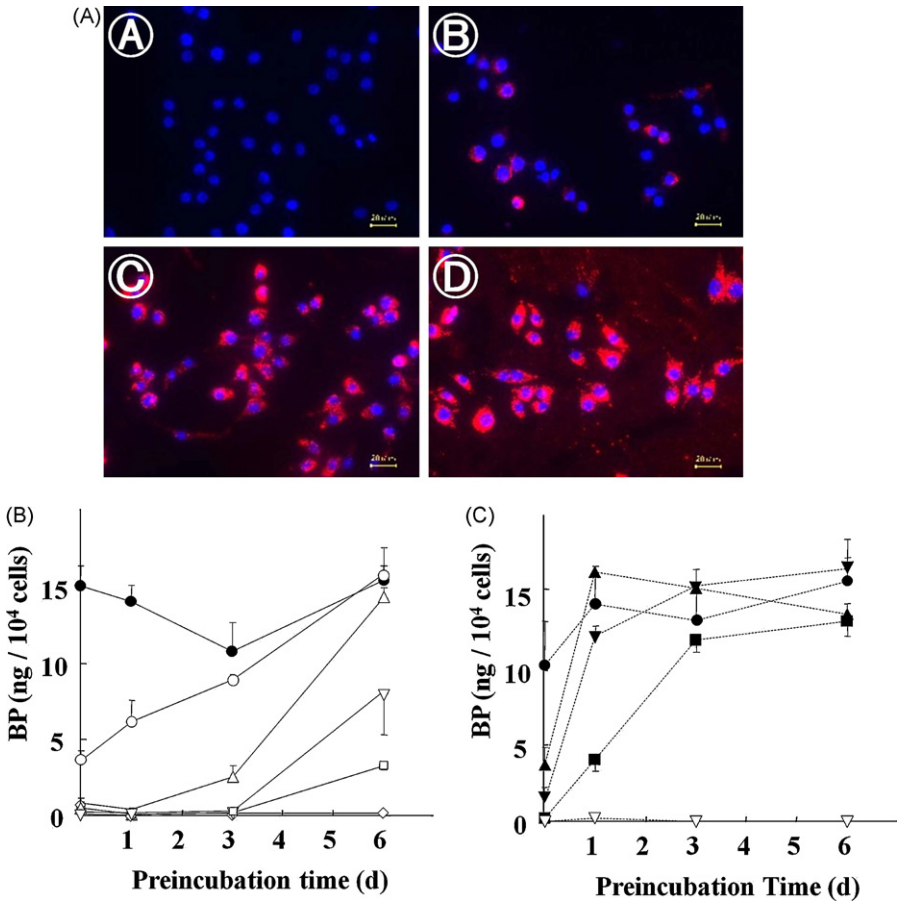

Fig. 2. Internalizaiton of nanoparticles into RAW 264.7 cells. (A) Fluorescence images of RAW264.7 cells incubated with rhodamine-labeled nanoparticles. (A) Type A nanoparticles in 10% serum for 3 h. (B) Type A nanoparticles (preincubated in 50% serum for 3 d) in 10% serum for 3 h. (C) Type NS nanoparticles in 10% serum for 3 h. (D) Type NS nanoparticles without serum for 3 h. Blue shows nuclei stained by Hoechst 33258, and red shows rhodamine-labeled nanoparticles. Scale bars indicate 20 μm. (B and C) Determination of internalized BP into RAW264.7 cells. Nanoparticles were preincubated in FBPBS solution (50%, v/v) at 37 °C for 1, 3, or 6 d prior to the assay. Each data point and bar represents the mean and S.D. of 6 wells. (B) PLA(6)/PEG(6)-PLA(9)-based nanoparticles. (C) PLA(6)/PEG(6)-PLGA(10)-based nanoparticles.

cles ($p < 0.01$). Extended residence in the blood might indicate low liver uptake, and vice versa. Nanoparticles did not accumulate in the muscles, kidneys, or lungs (data not shown).

Interestingly, only the type A nanoparticles had a tendency to accumulate in the spleen, although previous reports have described the accumulation of some nanoparticles in the bone marrow and lymph nodes (Manolova et al., 2008). The mechanism of splenic accumulation is not yet known, although it has been suggested

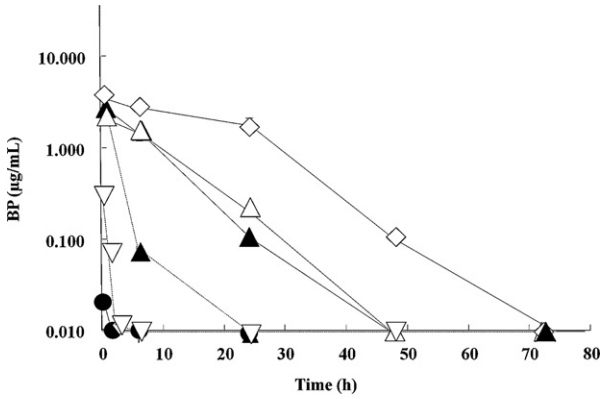

Fig. 3. Blood clearance profiles of nanoparticles in ddY mice. The concentration of betamethasone (BP) in the blood is shown. Each data point represents the mean ($n = 5$). S.D. is within 5% of the mean. Half-life of each nanoparticle is as follows: type A, 7.8 h; type B, 25.2 h; type C, 3.2 h; type D, 5.8 h; type NS, <10 min.

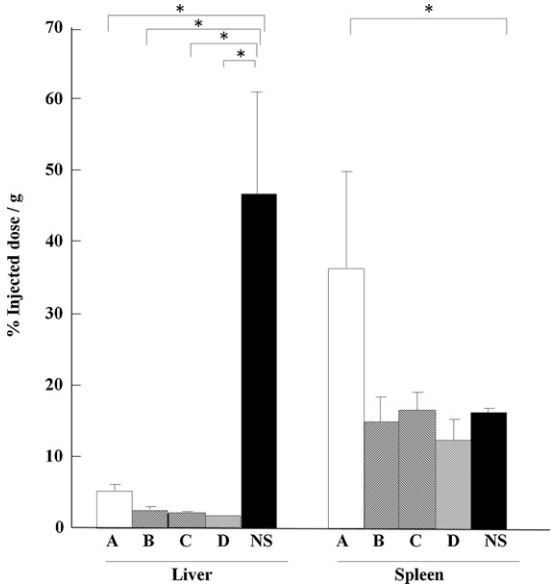

Fig. 4. Biodistribution of BP 24 h after i.v. administration to mice. The % injection dose/g tissue is shown. Columns and bars represent the mean and S.D. ($n = 4$). Type A, open bars; type B, forward slash; type C, back slash; type D, cross-hatched; type NS, closed bars. *$p < 0.01$.

that reduced liver uptake might lead to increased spleen capture of PEGylated PLA and PLGA particles. It has been reported that nanoparticles with a diameter of less than 70 nm reach tissues more efficiently than larger nanoparticles and therefore have a reduced half-life in the blood (Stolnik et al., 2001). Those nanoparticles might also pass through the sinusoidal fenestrations in the liver, resulting in hepatic accumulation, whereas blended nanoparticles with a 51-nm diameter (type B) did not show such tendency in this study. Further study is also necessary to define the distribution of type C nanoparticles, since it was cleared from the blood relatively early but did not accumulate in the liver or spleen. They might have been quickly degraded and excreted.

4. Conclusion

In this study various types of nanoparticles encapsulating BP were prepared from mixtures of PLA/PLGA homopolymers and PEG-PLA/PLGA block copolymers at various blend ratios. Our results indicate that the properties of blended nanoparticles can be controlled by changing the compositions/molecular weight of the PLA/PLGA homopolymers and the blend ratio of block copolymers and homopolymers. From the systematic evaluation of BP release behavior and interactions with macrophage-like cells, it appears that the nanoparticles initially release PEG from their surfaces, resulting in increased internalization by cells and a subsequent gradual release of BP. These studies will be useful in the design and optimization of long-circulating, intravenously injectable, biodegradable nanoparticles that encapsulate drugs. The therapeutic activity of various nanoparticles encapsulating BP is now under investigation on experimental arthritic animal models.

Acknowledgements

We thank Shionogi & Co., Ltd. for supplying the TR-FIA assay kit and Ms Yoshie Ishii for her technical assistance.

References

Anderson, J.M., Shive, M.S., 1997. Biodegradation and biocompatibility of PLA and PLGA microspheres. Adv. Drug Deliv. Rev. 28, 5–24.
Astete, C.E., Sabliov, C.M., 2006. Synthesis and characterization of PLGA nanoparticles. J. Biomater. Sci. Polym. Ed. 17, 247–289.
Avgoustakis, K., Beletsi, A., Panagi, Z., Klepetsanis, P., Karydas, A.G., Ithakissios, D.S., 2002. PLGA-mPEG nanoparticles of cisplatin: in vitro nanoparticle degradation, in vitro drug release and in vivo drug residence in blood properties. J. Control. Rel. 79, 123–135.
Avgoustakis, K., Beletsi, A., Panagi, Z., Klepetsanis, P., Livaniou, E., Evangelatos, G., Ithakissios, D.S., 2003. Effect of copolymer composition on the physicochemical characteristics, in vitro stability, and biodistribution of PLGA-mPEG nanoparticles. Int. J. Pharm. 259, 115–127.
Avgoustakis, K., 2004. Pegylated poly(lactide) and poly(lactide-co-glycolide) nanoparticles: preparation, properties and possible applications in drug delivery. Curr. Drug Deliv. 1, 321–333.
Bazile, D., Prud'homme, C., Bassoullet, M.T., Marlard, M., Spenlehauer, G., Veillard, M., 1995. Stealth Me, PEG-PLA nanoparticles avoid uptake by the mononuclear phagocytes system. J. Pharm. Sci. 84, 493–498.
Beletsi, A., Panagi, Z., Avgoustakis, K., 2005. Biodistribution properties of nanoparticles based on mixtures of PLGA with PLGA-PEG diblock copolymers. Int. J. Pharm. 298, 233–241.
Feng, S.S., 2004. Nanoparticles of biodegradable polymers for new-concept chemotherapy. Expert Rev. Med. Devices 1, 115–125.
Gref, R., Minamitake, Y., Peracchia, M.T., Trubetskoy, V., Torchilin, V., Langer, R., 1994. Biodegradable long-circulating polymeric nanospheres. Science 263, 1600–1603.
Gref, R., Miralles, G., Dellacherie, E., 1999. Polyoxyethylene-coated nanospheres: effect of coating on zata potential and phagocytosis. Polym. Int. 48, 251–256.
Gref, R., Luck, M., Quellec, P., Marchand, M., Dellacherie, E., Harnisch, S., Blunk, T., Muller, R.H., 2000. 'Stealth' corona-core nanoparticles surface modified by polyethylene glycol (PEG): influences of the corona (PEG chain length and surface density) and of the core composition on phagocytic uptake and plasma protein adsorption. Colloids Surf. B: Biointerfaces 18, 301–313.
Gref, R., Quellec, P., Sanchez, A., Calvo, P., Dellacherie, E., Alonso, M.J., 2001. Development and characterization of CyA-loaded poly (lactic acid)–poly (ethylene glycol)PEG micro- and nanoparticles. Comparison with conventional PLA particulate carriers. Eur. J. Pharm. Biopharm. 51, 111–118.
Higaki, M., Ishihara, T., Izumo, N., Takatsu, M., Mizushima, Y., 2005. Treatment of experimental arthritis with poly(D,L-lactic/glycolic acid) nanoparticles encapsulating betamethasone sodium phosphate. Ann. Rheum. Dis. 64, 1132–1136.
Ishihara, T., Izumo, N., Higaki, M., Shimada, E., Hagi, T., Mine, L., Ogawa, Y., Mizushima, Y., 2005. Role of zinc in formulation of PLA/PLGA nanoparticles encapsulating betamethasone phosphate and its release profile. J. Control. Rel. 105, 68–76.
Ishihara, T., Takahashi, M., Higaki, M., Takenaga, M., Mizushima, T., Mizushima, Y., 2008. Prolonging the in vivo residence time of prostaglandin E1 with biodegradable nanoparticles. Pharm. Res. 25, 1686–1695.
Ishihara, T., Takahashi, M., Higaki, M., Mizushima, Y., 2009. Efficient encapsulation of a water-soluble corticosteroid in biodegradable nanoparticles. Int. J. Pharm. 365, 200–205.
Maeda, H., Wu, J., Sawa, T., Matsumura, Y., Hori, K., 2000. Tumor vascular permeability and the EPR effect in macromolecular therapeutics: a review. J. Control. Rel. 65, 271–284.
Manolova, V., Flace, A., Bauer, M., Schwarz, K., Saudan, P., Bachmann, M.F., 2008. Nanoparticles target distinct dendritic cell populations according to their size. Eur. J. Immunol. 38, 1404–1413.
Moghimi, S.M., Hunter, A.C., Murray, J.C., 2001. Long-circulating and target-specific nanoparticles: theory to practice. Pharm. Res. 53, 283–318.
Mosqueira, V.C., Legrand, P., Morgat, J.L., Vert, M., Mysiakine, E., Gref, R., Devissaguet, J.P., Barratt, G., 2001. Biodistribution of long-circulating PEG-grafted nanocapsules in mice: effects of PEG chain length and density. Pharm. Res. 18, 1411–1419.
Nguyen, C.A., Allemann, E., Schwach, G., Doelker, E., Gurny, R., 2003. Cell interaction studies of PLA-MePEG nanoparticles. Int. J. Pharm. 254, 69–72.
Okada, H., Toguchi, H., 1995. Biodegradable microspheres in drug delivery. Crit. Rev. Ther. Drug Carrier Syst. 12, 1–99.
Panyam, J., Zhou, W.Z., Prabha, S., Sahoo, S.K., Labhasetwar, V., 2002. Rapid endo-lysosomal escape of poly(DL-lactide-co-glycolide) nanoparticles: implications for drug and gene delivery. FASEB J. 16, 1217–1226.
Peer, D., Karp, J.M., Hong, S., Farokhzad, O.C., Margalit, R., Langer, R., 2007. Nanocarriers as an emerging platform for cancer therapy. Nat. Nanotechnol. 2, 751–760.
Peracchia, M.T., 2003. Stealth nanoparticles for intravenous administration. S. T. P. Pharma Sci. 13, 155–161.
Quellec, P., Gref, R., Dellacherie, E., Sommer, F., Tran, M.D., Alonso, M.J., 1999. Protein encapsulation within poly(ethylene glycol)-coated nanospheres. II. Controlled release properties. J. Biomed. Mater. Res. 47, 388–395.
Riley, T., Stolnik, S., Heald, C.R., Xiong, C.D., Garnett, M.C., Illum, L., Davis, S.S., 2001. Physicochemical evaluation of nanoparticles assembled from poly(lactic acid)-poly(ethylene glycol)(PLA-PEG)block copolymers as drug delivery vehicles. Langmuir 17, 3168–3174.
Sakai, T., Kohno, H., Ishihara, T., Higaki, M., Saito, S., Matsushima, M., Mizushima, Y., Kitahara, K., 2006. Treatment of experimental autoimmune uveoretinitis with poly(lactic acid) nanoparticles encapsulating betamethasone phosphate. Exp. Eye Res. 82, 657–663.
Sasatsu, M., Onishi, H., Machida, Y., 2006. In vivo and vivo characterization of nanoparticles made of MeO-PEG amine/PLA block copolymer and PLA. Int. J. Pharm. 317, 167–174.
Stolnik, S., Dunn, S.E., Garnett, M.C., Davies, M.C., Coombes, A.G., Taylor, D.C., Irving, M.P., Purkiss, S.C., Tadros, T.F., Davis, S.S., 1994. Surface modification of poly(lactide-co-glycolide) nanospheres by biodegradable poly(lactide)-poly(ethylene glycol) copolymers. Pharm. Res. 11, 1800–1808.
Stolnik, S., Heald, C.R., Neal, J., Garnett, M.C., Davis, S.S., Illum, L., Purkis, S.C., Barlow, R.J., Gellert, P.R., 2001. Polylactide-poly(ethylene glycol) micellar-like particles as potential drug carriers: production, colloidal properties and biological performance. J. Drug Target. 9, 361–378.
Torchilin, V.P., 2005. Recent advances with liposomes as pharmaceutical carriers. Nat. Rev. Drug Discov. 4, 145–160.
Torchilin, V.P., 2007. Micellar nanocarriers: pharmaceutical perspectives. Pharm. Res. 24, 1–16.
Vonarbourg, A., Passirani, C., Saulnier, P., Benoit, J.P., 2006. Parameters influencing the stealthiness of colloidal drug delivery systems. Biomaterials 27, 4356–4373.
Yih, T.C., Al-Fandi, M., 2006. Engineered nanoparticles as precise drug delivery systems. J. Cell. Biochem. 97, 1184–1190.
Yoo, H.S., Park, T.G., 2001. Biodegradable polymeric micelles composed of doxorubicin conjugated PLGA-PEG block copolymer. J. Control. Rel. 70, 63–70.
Zambaux, M.F., Bonneaux, F., Gref, R., Dellacherie, E., Vigneron, C., 1999. MPEO-PLA nanoparticles: effect of MPEO content on some of their surface properties. J. Biomed. Mater. Res. 44, 109–115.